ELSEVIER

Biophysical Chemistry 129 (2007) 190–197

Biophysical Chemistry

http://www.elsevier.com/locate/biophyschem

# Towards understanding structure-stability and surface properties of laminin peptide YIGSR and mutants

Muthuselvi Lakshmanan, Aruna Dhathathreyan *

*Chemical Lab., CLRI, Adyar, Chennai 600 020, India*

Received 26 March 2007; received in revised form 30 May 2007; accepted 30 May 2007
Available online 7 June 2007

**Abstract**

Properties of laminin peptide YIGSR and its mutated sequences YIGSD, YIGSS, YIGSN and YIGSQ have been investigated using molecular dynamics simulations (MDS) and Langmuir films at air/water interface. Simulation studies on laminin peptide YIGSR were performed in the isothermal–isobaric (N, P, T) ensemble, with run up to 5 ns in water as well as lipid environment at 298 K. From different initial configurations, shape transformations of the peptides on the timescale of nanoseconds were observed. The results showed YIGSR to be the most stable peptide with the order of minimized energy being YIGSR<YIGSQ<YIGSD<YIGSN<YIGSS. Subsequent experiments with newly synthesized amphiphilic derivatives of the mutated peptides were carried out for their monolayer formation and stability at air/water interface using surface pressure–molecular area ($\pi$–$A$) and surface potential–molecular area ($\Delta V$–$A$) isotherms. The surface and interface activity of these compounds followed a similar trend as with the MDS studies. Results suggest that single amino acid mutation leads to large changes in minimized energy, surface activity and different rates to reach stable conformation. The native YIGSR is the most stable sequence with highest surface activity while YIGSS is least stable and has the lowest surface activity. This corroborated the results of the MDS.


*Keywords:* Laminin peptides; Langmuir films; Molecular dynamics simulation; Interface

## 1. Introduction

The process of peptide folding [1,2] and their organization in solution has been used to mimic highly functional and dynamic structures in biology [3,4]. Though a number of papers have appeared in the literature in the recent years on self assembly processes in biomolecules [5–7], designing a supra-molecular structure is still difficult. Theoretical approaches to predict the (stable) folded structure of a peptide and the process of peptide folding fall into three categories; statistical approaches, conformational search methods and dynamics simulation [8]. Of these, dynamics simulation methods, such as molecular dynamics (MD), have been used to characterize particular folded states in solution [9–12].

In nature self assembly processes take place resulting in complex hierarchical order, many researchers have designed novel materials by mimicking these natural self-assembled processes. The first step here is to develop molecular building blocks, which are able to self-assemble into highly ordered structures. Recently, there has been an effort to mimic essential properties of natural extracellular matrix (ECM) [13]. ECM is a viscoelastic network, which consists of nanofibrous proteins like collagen, laminin and elastin to provide biological and chemical moieties as well as physical frameworks for cells. Mimicking the ECM might be the best route to develop next generation materials, which allow control over cell adhesion, migration, proliferation and differentiation. Muthuselvi and Dhathathreyan have studied the self assembly processes in laminin peptides [14] and have estimated the hydrodynamically coupled water in these peptides [15]. Laminin is a major component of the extracellular matrix that has been shown to exhibit many biological activities with various cell types, including neuronal cells [16]. The interaction of laminin with several primary and established cell lines derived from the peripheral and central nervous systems, has been shown to

* Corresponding author. Tel.: +91 44 24411630; fax: +91 44 24911589.
*E-mail address:* aruna@clri.info (A. Dhathathreyan).

0301-4622/$ - see front matter © 2007 Elsevier B.V. All rights reserved.
doi:10.1016/j.bpc.2007.05.019

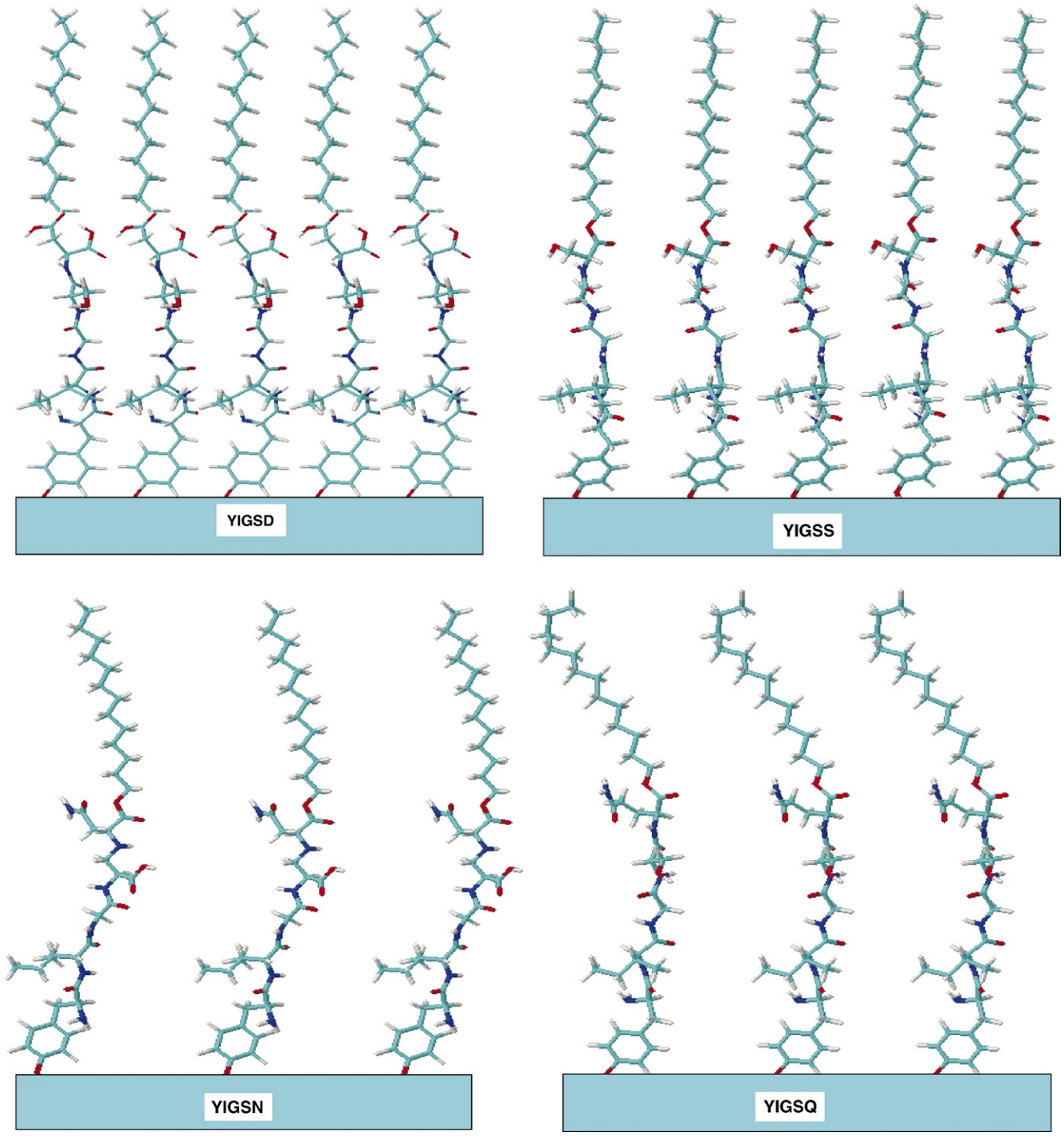


Fig. 1. Energy minimized structures of YIGSD,YIGSS,YIGSN and YIGSQ.

result in increased cellular adhesion and neurite outgrowth [16–18].

The synthetic analogues of laminin peptides YIGSR and IKVAV have found widespread interest in cancer research towards preventing tumor metastasis [19–21]. Computer simulation studies of YIGSR-containing sequences have been previously reported [22–24]] wherein the inspiration was the potential application of laminin-derived fragments towards developing novel drugs against tumor metastasis.

Brandt-Rauf et al. [22] and McKelvey et al. [23] studied the pentapeptide YIGSR, whereas Ostheimer et al. [24] studied the nonapeptide CDPGYIGSR.

Makholiso and Melchionna studied the molecular properties of the laminin-derived oligopeptide, H–CDPGYIGSR–NH2, in aqueous medium as well as in the immobilized state on a solid using computer simulation and experimental approach [25]. This work showed the important role played by the terminal arginine in the overall conformation of the oligopeptides.

In the present study, molecular dynamics simulation (MDS) on the folding of the laminin peptide YIGSR and the sequences mutated in the 5th position with amino acids *D*, *S*, *N* and *Q* in water and in a lipid environment have been presented. The lipid environment has been chosen to mimic the cell membrane. From the minimized energy values obtained a trend in the overall activity of the native peptide and the sequences YIGSD, YIGSS, YIGSN and YIGSQ have been evaluated. In order to develop probable peptide carriers, amphiphilic derivatives of the above sequences have been synthesized and their ability to assemble as Langmuir monolayers at air/water interface and in LB films investigated. Here the choice of *D*, *S*, *N* and *Q* was based on the fact that in the hydropathy scale of amino acids *R* *D*, *S*, *N* and *Q* show nearly similar polarity values. Thus one does not expect drastic changes in the overall amphiphilicity of the sequences. Monomolecular lipid films at the air/water interface serve as good models for interaction of peptides with membranes and do not have the disadvantages of small curvature radius of small unilamellar vesicles (SUVs). Films of the amphiphilic peptides prepared in this study as Langmuir films have been transferred onto solid substrates using the Langmuir–Blodgett film (LB film) technique.

## 2. Experimental

### 2.1. Molecular dynamics simulation

#### 2.1.1. Force field

The structural properties of the native peptide YIGSR and mutated YIGSD, YIGSS, YIGSQ and YIGSN have been investigated using MDS for a total simulation time of 5 ns, performed using AMBER9 [26]. The effects of simulation protocols and force fields have been analyzed using "ptraj" including hydrogen bonding, bond length and bond angle constraints by the usual standard procedure. Generalized Born/Surface Area (GB/SA) with implicit solvent model has been used for the calculations.

In this GB/SA model [27], the total solvation energy ($G_{solv}$) is given as the sum of a solvent-solvent cavity term ($G_{cav}$), a solute–solvent van der Waals term ($G_{vdW}$) and a solute–solvent electrostatic polarization term ($G_{pol}$):

$$G_{solv} = G_{cav} + G_{vdW} + G_{pol}.$$

The minimization for peptides-native YIGSR and mutated YIGSD, YIGSS, YIGSN and YIGSQ in implicit water and the phospholipid dipalmitoylphosphatidyl choline (DPPC) were carried out for 5 ns each on an 800 MHz Duron processor in a personal computer.

### 2.2. Synthesis of amphiphilic derivatives of the peptides

The pentapeptides YIGSS, YIGSN, YIGSD and YIGSQ were obtained from Ezbiolab., USA, and were 99.9% pure. The hydrophobic residue myristoyl was incorporated to all the above peptide sequences as the corresponding fatty acid using benzotriazole-1-yl-oxy-tris-(dimethylamino)-phosphonium (BOP)/DIEA (*N*,*N*_-diisopropylethylamine) in dimethyl formamide (DMF) as the activating agent. YIGSS-myristoyl (YIGSSmyr), YIGSN-myristoyl (YIGSN-myr), YIGSD-myristoyl (YIGSR-myr) and YIGSQ-myristoyl (YIGSQ-myr) were synthesized and were characterized by amino acid analysis, mass spectrometry electrospray, and reverse phase (RP)-HPLC (C8), and were purified when necessary by preparative HPLC-C8. Here the C8 is used in the stationary phase because the peptides have some degree of hydrophobicity and thus can help in resolving different peptides of varying polarity. Further methanol was used as solvent to carry out the MS analysis. The purity of the samples was checked by HPLC, being in all cases higher than 98% (calculated from peak area) and mass spectra indicated the only presence of molecular peaks. Nevertheless, before use, peptide samples were repeatedly washed with cold diethyl ether and *n*-hexane in order to remove traces of hydrophobic impurities that could interfere in the physico-chemical studies. Using norleucine (nle) as the internal standard peptide concentrations in their standard solutions were determined by quantitative amino acid analysis.

The structures of the amphiphilic derivatives are given in Fig. 1. These were arrived at by first minimizing single molecules of the various peptides and then docking them on to a surface.

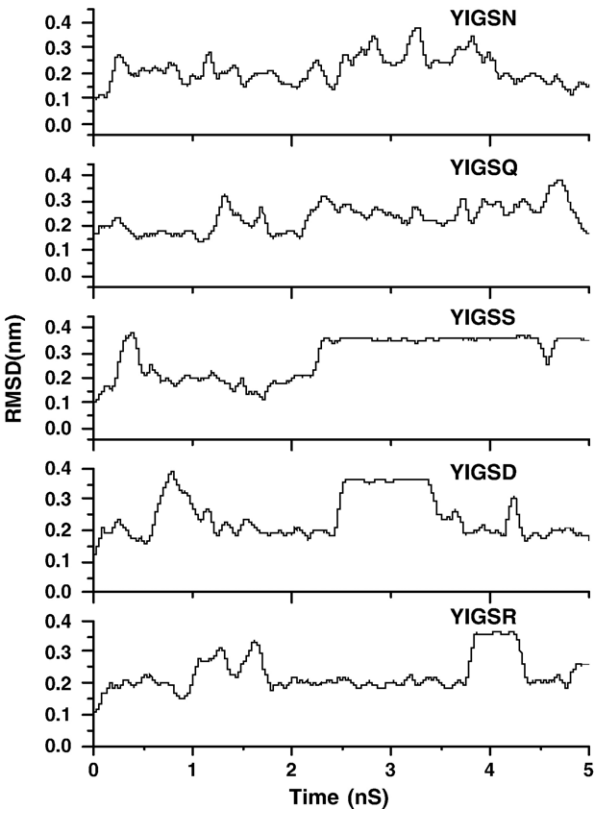


Fig. 2. Plots of RMSD against Time for the native peptide YIGSR and the mutated sequences.

### 2.3. Compression isotherms

The monolayer properties of the amphiphilic peptides at air/buffer interface were characterized using a NIMA 601 S single barrier trough (Wilhelmy balance) containing 530 ml of physiological buffer solution (PBS). The barrier compressed the monolayer at a speed of 10 $cm^2$/min. Peptide solutions of $10^{-3}$ M in chloroform: methanol (vol ratio 3:1) were spread on PBS subphases and surface pressure was continuously recorded during film compression. CD spectra of the pure peptides in water were compared with that of the films of amphiphilic derivatives obtained from the above Langmuir films. There were no dramatic changes in the secondary structures indicating that the amphiphilic peptides were stable. Each $\pi$–$A$ curve shown represents an average of the measurement of two or three separate compression processes of newly spread monolayers. Experiments were carried out at 21±0.5 °C. The surface potential was measured using a Kelvin vibrating plate method [28]. The accuracy in surface potential values was 0.1 V. The surface potential $\Delta V$ was measured as a difference between potential of a pure water surface and that of water surface covered with a monolayer. From the experimental $\Delta V$ values the dipole moment component $\mu\perp$ (normal component of dipole moment value) are estimated from the Helmholtz equation

$$\mu \perp = \varepsilon_0 A \Delta V$$

Here $\Delta V$ and $A$ are the surface potential and average area of a close-packed monolayer and $\varepsilon_0$ is the permittivity of free space.

### 2.4. FTIR spectra of Langmuir films

#### 2.4.1. FTIR spectra of Langmuir films using photoelastic modulated (PEM)-FTIR

The measurements of PEM-FTIR was carried out with a Brucker IF S48 spectrometer using ZnSe photoelastic modulator (Hinds type II) and two ZnSe plates at Brewster incidence. The frequencies of the methylene stretching vibration modes have been previously used as an indication of the ordered states of the packing of the monolayer in the condensed state. The frequencies, shapes and intensities of the infrared C–H stretching bands provide information on the orientation, conformation and packing of the hydrocarbon chain in the monolayer. The $v_{as}$ $CH_2$ (asymmetric) and $v_s$ $CH_2$ (symmetric) bands appearing in the spectrum correspond to a preferential in-plane orientation of transition moments which is consistent with the alkyl chains quasi perpendicular to the interface. The signals from the hydrophilic groups immersed in water being weak cannot be observed directly in the spectrum. Hence only the bands corresponding to the long alkyl chains are indicated here [29]. For different molecular areas during compression of the monolayer, the $v_{as}$ and $v_s$ $CH_2$ bands were recorded.

## 3. Results and discussion

Fig. 2 shows the plots of RMSD values for the peptides versus time (ns).

Because of the large number of configurations that are possible for such short peptides the convergence in the properties cannot be considered rigorously. However for the MDS for 5 ns carried out it is seen that YIGSQ has the least difference in RMSD (0.18 nm) from the initial state while YIGSS has the highest (0.32 nm). Also YIGSS shows an initial lowering of the RMSD up to about 2.5 ns after which it starts to rise and then levels off at 0.32 nm.

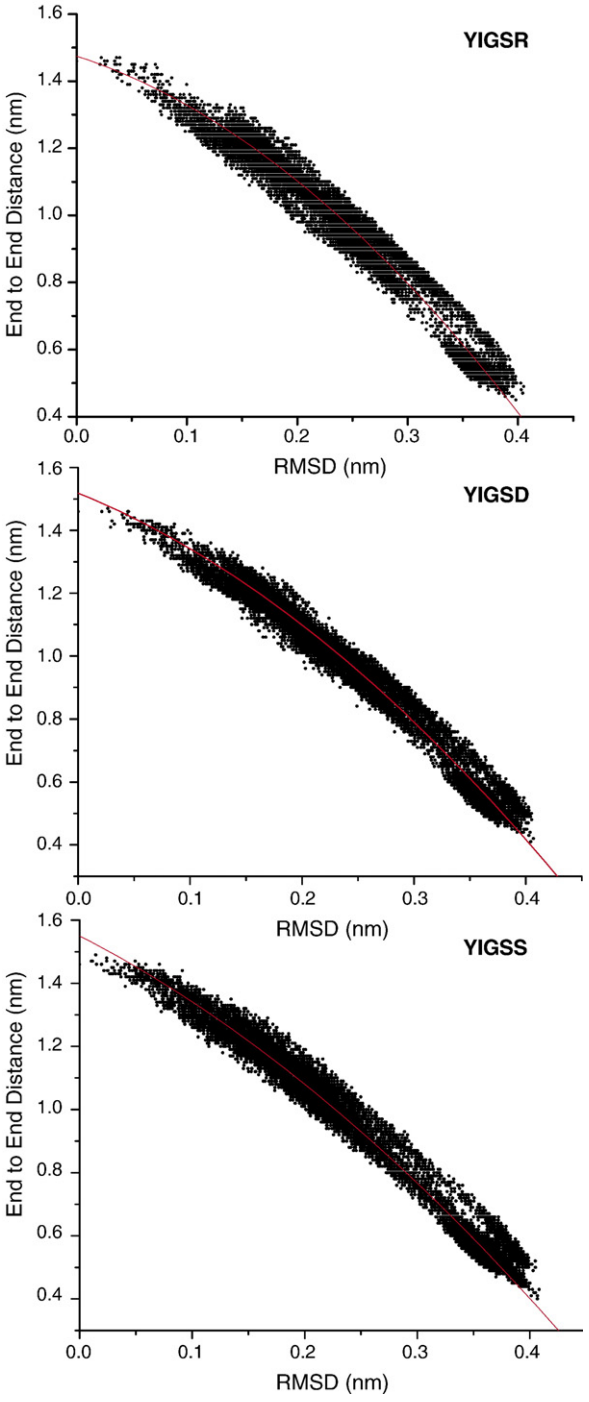


Fig. 3. Plots of End to end distance versus RMSD for the native peptide YIGSR and the mutated sequences (Fitted to polynomial of second degree).

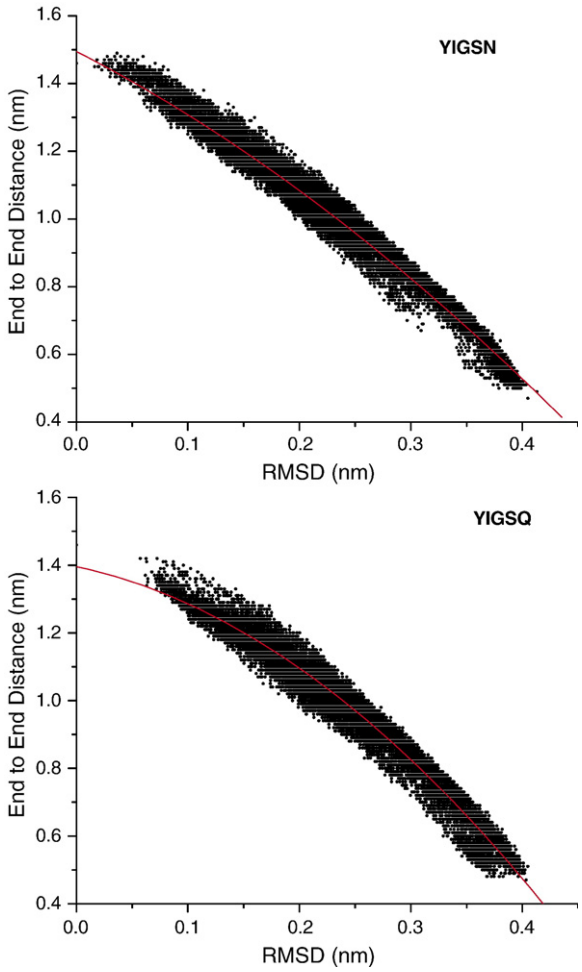


Fig. 3 (*continued*).

All other peptides do not show large deviations as a function of time.

Fig. 3 Shows the end to end distance as a function of RMSD values for YIGSR and the mutated peptides evaluated over a time trajectory of 5 ns.

These plots show the stability of the peptides as is seen by the shortest end to end distance. Here the order is seen as $Q>R>D>N>S$. The plots were fitted to a polynomial of second degree of the form

$$Y = A + B_1X + B_2X^2$$

and the values of coefficients and the $R$ value are given in Table 1.

Generally in the energy minimization with MDS, Potential energy, torsional angles, and hydration of the polar head groups under periodic boundary conditions (PBC) are used. The potential energy is partitioned explicitly for a single molecule orientation potential, dipolar couplings, rotational–rotational, translational–rotational, and translational–translational interactions. The final potential energy of the molecules consists of diagonal terms corresponding to bond length deforrmation, valence angles, torsional angles and out of plane interactions, off-diagonal or cross terms, and nonbonded interactions. In this the major contribution arises from the first three terms, especially the bond bond interactions. In the case of short peptides studied here these interactions contribute maximum to the energy. Thus the changes in end to end distances of the peptides in the final structures in this study are of importance to the overall stability.

Hence the $B_1$ values are indicative of the rate at which minimum end to end distance is reached for a particular RMSD From the $B_1$ listed in Table 1,it is seen that $Q$ has the lowest value and $S$ the highest with $Q<R<D<N<S$. The corresponding minimized energy values for the native laminin peptide YIGSR and the mutated sequences on hydration and with the phospholipid DPPC are given in Table 2.

It is seen that the laminin peptide in its native form has the lowest energy in both water as well as with DPPC. The energy values for the different peptides cannot be compared absolutely. However the differences in energy between the mutated peptides and the native YIGSR may be relevant for this study.

The order of stability from these values is as $R>Q>D>N>S$ for both aqueous and lipid environment. A comparison of the energy values of the peptides in hydrated condition and in lipid environment showed that the peptides are relatively more stable in the aqueous phase.

Coupled water fractions in amino acids and peptides from our earlier study showed a direct correlation to the degree of polarity of the residues. These values were estimated from the side chain contributions of the amino acids. In the case of energy calculations, the whole peptide including the backbone is taken into account. The evaluated coupled water fractions for the YIGSD, YIGSS and YIGSN showed the same trend as in the energy-minimized values in this study the exceptions being YIGSR and YIGSQ. This may be due to variations in backbone conformation for the peptide bonds $S$–$R$ and $S$–$Q$ in these 2 peptides. In the minimized energy conformations of YIGSR and YIGSQ (peptide bond $S$–$R$ and $S$–$Q$) small differences with $\varphi = -10.54°$ and $-13.61°$ for $Q$ and $R$ are seen. This indicates that even such small change in φ can lead to large changes in energy values between YIGSR and YIGSQ. The surface activity and interfacial properties of amphiphilic derivatives of YIGSR and its mutants were studied using their Langmuir films

Table 1

| Peptide | $A$ | $B_1$ | $B_2$ | $R$ (regression coefficient) |
|---|---|---|---|---|
| YIGSR | 14.74921 | −1.06326 | −0.39828 | 0.96964 |
| YIGSD | 15.18782 | −1.44212 | −0.32784 | 0.98144 |
| YIGSS | 15.5041 | −1.82827 | −0.2607 | 0.98366 |
| YIGSQ | 13.96012 | −0.6943 | −0.40229 | 0.96522 |
| YIGSN | 14.95229 | −1.69273 | −0.18149 | 0.97082 |

Table 2

| Peptides | Water (Kcal/mol) | DPPC (Kcal/mol) | Coupled water fraction[15] |
|---|---|---|---|
| YIGSR | −251.622 | −193.252 | 0.432 |
| YIGSD | −127.647 | −74.266 | 0.413 |
| YIGSS | −94.932 | −62.326 | 0.407 |
| YIGSN | −123.299 | −89.23 | 0.425 |
| YIGSQ | −144.729 | −115.197 | 0.437 |

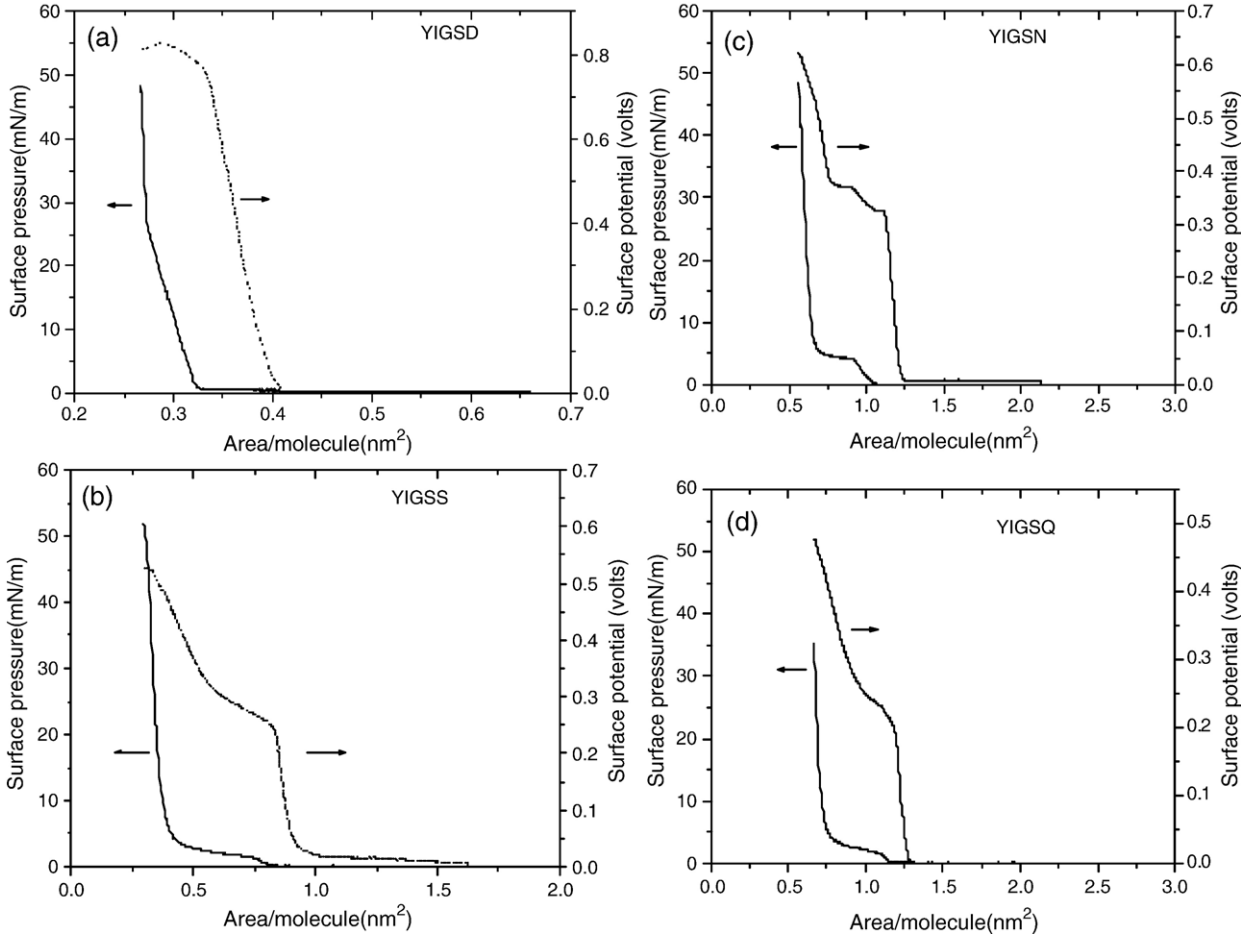


Fig. 4. Surface pressure and surface potential against molecular area ($\pi$–$A$ and $\Delta V$-A) for (a) YIGSD-myr; (b)YIGSS-myr; (c)YIGSN-myr; (d) YIGSQ-myr on deionized water subphase, $T$=22 °C.

at air/water interface. Fig. 4a–d give the plots of $\pi$–$A$ (surface pressure–molecular area) and $\Delta V$–$A$ (surface potential-molecular area) isotherms of the amphiphilic derivatives YIGSS-myr, YIGSD-myr, YIGSQ-myr and YIGSN-myr. From the isotherms, it is seen that all the compounds show 2 d gaseous to liquid expanded (LE) states and in some cases also the liquid condensed (LC) state. The different phases in the isotherms are identified from the compressibility modulus $C_s^{-1}$ defined as $-A(\partial\pi/\partial A)$. The maximum collapse pressure, which is a measure of the surface activity of the compound, can also be determined by this parameter [30].

Generally $C_s^{-1}$ values lower than 12.5 mN/m are attributed to the gaseous state, values between 12.5 and 100 mN/m to liquid expanded state, 100 to 250 mN/m to the liquid condensed state while $C_s^{-1}$ values greater than 250 mN/m are assigned to the solid state of the film. At the collapse pressure the value approaches zero. Based on the above criterion, it is seen that in case of YIGSD-myr, there is a change in $C_s^{-1}$ value from 10.6 to 156 to 298 as the pressure increases from 0.5 to 1.5 to 25.5 mN/m suggesting that the monolayer goes through a gaseous to LE to LC phase. For peptide derivatives YIGSN-myr, YIGSS-myr and YIGSQ-myr the transition between the LE to LC phase occurs around 4.14, 2.5, 3.06 mN/m as is seen from the $C_s^{-1}$ values. In these three peptides this seems to suggest it is a first order transition whereas in the case of YIGSD-myr this transition does not exist. This could be due to the fact that YIGSD-myr packs most compactly at air/water interface compared to the other amphiphiles due to less curved segments in the tail. For the minimized structures of the peptides (as given in Fig. 1), the projected areas are in close agreement with the experimentally determined area values. The area/molecule, the projected area obtained from the molecular models and the surface potential values are given in Table 3. The average area/molecule for the natural peptide sequence from the earlier study was found to be 0.402 nm$^2$/molecule [14] while the mutated sequences show areas ranging between 0.3 to 0.69 nm$^2$/molecule suggesting that the nature of the residue at the end determines the overall surface area at air/water interface.

Table 3

| Amphiphilic peptide | Area/molecule (nm$^2$) at $\pi$=25 mN/m | | Surface potential (volts) | Dipole moment $\mu_\perp$(debye) |
|---|---|---|---|---|
| | Experimental | Model | | |
| YIGSR-myr[14] | 0.402 | 0.38 | 0.59 | 0.619 |
| YIGSS-myr | 0.34 | 0.30 | 0.52 | 0.475 |
| YIGSN-myr | 0.61 | 0.59 | 0.59 | 0.963 |
| YIGSD-myr | 0.28 | 0.25 | 0.81 | 0.607 |
| YIGSQ-myr | 0.69 | 0.70 | 0.47 | 0.868 |

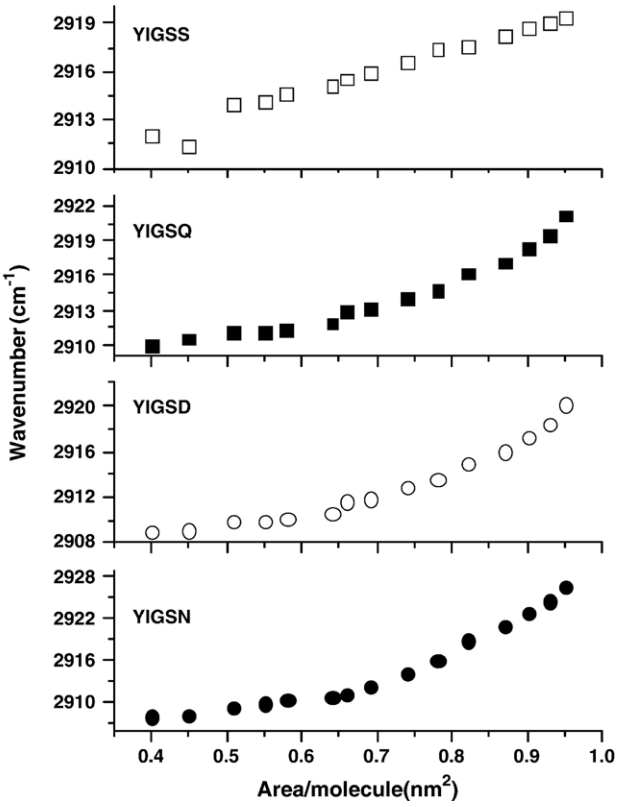


Fig. 5. Plot of wave numbers of $\nu_{as}$ methylene stretching vibrations against area per molecule of 1-YIGSN-myr, 2-YIGSD-myr, 3-YIGSQ-myr, and 4-YIGSS-myr.

From Fig. 1, which shows the energy, minimized structures of the peptides at the interface, the projected areas at the air/water interface agree quite well with the experimentally measured values. The native sequence YIGSR-myr and the mutated peptide YIGSD-myr show nearly the same area while the others show large changes in the area, potential and dipole moment values.

The area/molecule from the models are slightly smaller than the experimentally measured values. This is due to the fact that the model takes into account single molecules at the interface whereas in the experiments, the packing is influenced by both intermolecular interactions as well as interaction of the polar groups with water.

From the $\mu\perp$ values it is seen that the lowest value of 0.475 Debye is for YIGSS while YIGSN has the highest dipole moment. The maximum surface pressure exhibited by these peptides are in the order YIGSQ < YIGSD < YIGSN < YIGSS ($\pi = 35 < 47 < 49 < 52$ mN/m). These values indicate that there are large changes in the surface activity of the peptide YIGSR [14] on mutation with YIGSS being least surface active.

In order to check the packing of these compounds at the air/water interface and order in the alkyl chains during compression of the monolayers, a plot of molecular area versus the intensity of $\nu_{as}$ $CH_2$ are shown in Fig. 5. It has been reported that the $\nu_{as}$ $CH_2$ vibrations are sensitive to conformation and can be correlated with trans/gauche ratio of the hydrocarbon chain [29].

Normally lowering of wavenumbers are characteristic of highly ordered conformations with preferential all-trans characteristics, while the number of gauche conformers increases with increasing wavenumbers and width of the band. The increased wave number of the methylene stretching vibration for a gauche rotamer is caused by a coupling between the carbon atoms and the methylene–hydrogen, which due to interconversion around the C–C bond is positioned in the plane defined by the carbon atoms, resulting in an increased force constant for that C–H bond. In contrast, for an all-trans conformation all methylene hydrogens are out of the plane.

Fig. 5 shows that there is an overall decrease in the wave numbers as the films are compressed giving rise to an overall increase in order of the alkyl chains.

Thus the results from $\pi$–$A$ isotherms and the PEM FTIR results show that the gauche defects are almost nil in the packing of the long alkyl chains.

## 4. Conclusions

In conclusion, the results from MDS and the Langmuir films at air/water interface suggest that single amino acid mutation leads to large changes in minimized energy, surface activity and different rates to reach stable conformation. The native YIGSR is the most stable sequence with highest surface activity and the shortest end to end distance while YIGSS is least stable and has the lowest surface activity. Thus it may be possible to design peptide carriers with improved surface or interface properties that may find applications as drug carrier.

## Acknowledgement

One of the authors L.M. would like to thank the Lady Tata memorial Trust, Mumbai for the award of a research fellowship.

## References

[1] M. Karplus, E.I. Shakhnovich, Theoretical studies of protein folding thermodynamics and dynamics, in: T. Creighton (Ed.), Protein Folding, W. H. Freeman and Company, New York, 1992, pp. 127–196, Chapt. 4.
[2] S. Borman, b-Peptides: nature improved? Chem. Eng. News 75 (1997) 32–35.
[3] G.R. Marshall, D.D. Beusen, G.V. Nikiforovich, Peptide conformation: stability and dynamics, Peptides: Synthesis, Structures and Applications, Academic Press, San Diego, 1995, pp. 193–245.
[4] X. Daura, B. Jaun, D. Seebach, W.F. van Gunsteren, A.E. Mark, Reversible peptide folding in solution by molecular dynamics simulation, J. Mol. Biol. 280 (1998) 925–932.
[5] G.E. Schulz, A critical evaluation of methods for prediction of protein secondary structures, Annu. Rev. Biophys. Biophys. Chem. 17 (1988) 1–21.
[6] P.D. Thomas, K.A. Dill, Statistical potentials extracted from protein structures: how accurate are they? J. Mol. Biol. 257 (1996) 457–469.
[7] J.M. Troyer, F.E. Cohen, Simplified models for understanding and predicting protein structure, in: K.B. Lipkowitz, D.B. Boyd (Eds.), Reviews in Computational Chemistry, vol. 2, VCH Publishers, Inc., New York, 1991, pp. 57–80.
[8] J.M. Troyer, F.E. Cohen, Simplified models for understanding and predicting protein structure, Rev. Comput. Chem. 2 (1991) 57–80.

[9] D.J. Tobias, C.L. Brooks, Thermodynamics and mechanism of a helix initiation in alanine and valine peptides? Biochemistry 30 (1991) 6059–6070.
[10] L. Zhang, J. Hermans, Molecular dynamics study of structure and stability of a model coiled coil, Proteins 16 (1993) 384–392.
[11] W.F. Van Gunsteren, P.H. Hunenberger, H. Kovacs, A.E. Mark, C.A. Schiffer, Investigation of Protein Unfolding and Stability by Computer Simulation Philosophical Transactions: Biological Sciences, 348, No. 1323, Protein Folding , Apr. 29 1995, pp. 49–59.
[12] S. Sheriff, K.L. Constantine, Redefining the minimal antigen-binding fragment, Nat. Struct. Biol. 3 (1996) 733–736.
[13] M.P. Lutolf, J.A. Hubbel, Synthetic biomaterials as instructive extracellular microenvironments for morphogenesis in tissue engineering, Nat. Biotechnol. 23 (2005) 47–55.
[14] M. Lakshmanan, A. Dhathathreyan, Amphiphilic laminin peptides at air/water interface—effect of single amino acid mutations on surface properties, J. Colloid Interface Sci. 302 (2006) 95–102.
[15] M. Lakshmanan, A. Dhathathreyan, Hydrodynamically coupled water in surface adsorbed amino acids as a tool to study hydrated peptides, Biochim. Biophys. Acta (BBA)-Proteins Proteomics 1774 (2007) 138–145.
[16] H.K. Kleinman, G.C. Sephel, K.I. Tashiro, et al., Laminin in neuronal development, Ann. N.Y. Acad. Sci. 580 (1990) 302–310.
[17] P.C. Letourneau, L.C. Condic, D.M. Snow, Interactions of developing neurons with the extracellular-matrix, J. Neurosci. 14 (1994) 915–928.
[18] L. McKerracher, M. Chamoux, C.O. Arregui, Role of laminin and integrin interaction in growth cone guidance, Mol. Neurobiol. 12 (1996) 95–116.
[19] J. Graf, Y. Iwamoto, M. Sasaki, et al., Identification of an amino-acid sequence in laminin mediating cell attachment, chemotaxis, and receptor-binding, Cell 48 (1987) 989–996.
[20] J. Graf, R.C. Ogle, F.A. Robey, et al., A pentapeptide from the laminin-1 chain mediates cell-adhesion and binds the 67000-laminin receptor, Biochemistry 26 (1987) 6896–6900.
[21] K. Tashiro, G.C. Sephel, B. Weeks, et al., A synthetic peptide containing the IKVAV sequence from the A chain of laminin mediates cell attachment, migration, and neurite outgrowth, J. Biol. Chem. 264 (1989) 16174–16182.
[22] P.W. Brandt-Rauf, M.R. Pincus, R.P. Carty, et al., Conformation of the metastasis-inhibiting laminin pentapeptide, J. Protein Chem. 8 (1989) 149–157.
[23] D.R. McKelvey, C.L. Brooks, M. Mokotoff, A Charmm analysis of the conformations of the metastatis-inhibiting laminin pentapeptide, J. Protein Chem. 267 (1991) 25120–25128.
[24] G.J. Ostheimer, J.R. Starkey, C.G. Lambert, S.L. Helgerson, E.A. Dratz, NMR constrained solution structures for laminin peptide-11 analogs define structural requirements for inhibition of tumor-cell invasion of basement–membrane matrix, J. Biol. Chem. 267 (1992) 25120–25128.
[25] S.A. Makohlisoa, S. Melchionna, Molecular characterization of a laminin-derived oligopeptide with implications in biomimetic applications, Biophys. Chem. 89 (2001) 129–144.
[26] http://amber.scripps.edu/doc9/amber9.pdf.
[27] W.C. Still, A. Tempczyk, R.C. Hawley, T. Hendrickson, Semianalytical treatment of solvation for molecular mechanics and dynamics, J. Am. Chem. Soc. 112 (1990) 6127–6129.
[28] G.L. Gaines Jr., Insoluble Monolayers at Liquid Gas Interfaces, Wiley–Interscience, New York, 1966.
[29] V. Neumann, A. Gericke, H. Huhnerfuss, Comparison of enantiomeric and racemic monolayers of 2-hydroxyhexadecanoic acid by external infrared reflection–absorption spectroscopy, Langmuir 11 (1995) 2206–2212.
[30] M. Broniatowski, N.V. Romeu, P. Dynarowicz-Łaütka, Two-dimensional miscibility studies—the analysis of interaction between long-chain alcohols and semifluorinated alkanes, J. Phys. Chem. B 110 (2006) 3078–3087.